Catalysis Today 137 (2008) 283–287

Contents lists available at ScienceDirect

Catalysis Today

journal homepage: www.elsevier.com/locate/cattod

EPR studies on NO interaction with MoO_x/t-ZrO_2 catalysts obtained by slurry deposition

Andrzej Adamski [a,*], Zbigniew Sojka [a,b]

[a] Jagiellonian University, Faculty of Chemistry, Ingardena 3, 30-060 Krakow, Poland
[b] Regional Laboratory of Physicochemical Analyses and Structural Research, Ingardena 3, 30-060 Krakow, Poland

ARTICLE INFO

Article history:
Received 31 July 2007
Received in revised form 5 February 2008
Accepted 25 February 2008
Available online 9 April 2008

Keywords:
NO activation
MoO_x/t-ZrO_2
Slurry deposition
EPR
SCR NO_x

ABSTRACT

Variable temperature adsorption of nitric oxide on MoO_3 supported on tetragonal zirconia (MoO_x/t-ZrO_2), obtained by slurry deposition, was investigated by EPR spectroscopy. The influence of molybdenum loading and co-adsorbed oxygen on the adsorption process of NO was elucidated. Particular attention was devoted to redox character of NO activation. Another important aspect concerned is the nature of surface nitrosyl complexes of molybdenum and their thermal stability. The role of oxygen in NO transformation over catalyst surface was also discussed.

© 2008 Elsevier B.V. All rights reserved.

1. Introduction

Catalytic systems based on molybdena are widely applied in many processes such as hydrodesulphurization, oxidation and oxidative dehydrogenation, isomerization, metathesis and hydrogenolysis [1–3]. They also are used as important components of commercial catalysts for selective catalytic reduction of nitrogen oxides (SCR NO_x) [4,5]. Additives of MoO_3 extend the durability of SCR NO_x catalysts in the presence of sulphur or arsenic as well as improve their mechanical strength and thermal stability. It is also known that MoO_3 is used to increase the acidity of the SCR NO_x catalysts [4].

The redox properties of molybdena-containing catalysts are mainly determined by the molybdenum loading and by its specific interactions with the support, controlling molecular architecture of the surface oxomolybdenum species. Both the preparation method and the nature of support are very important, because of their strong influence on the interfacial processes involved in the MoO_3 deposition process. The majority of supported molybdenum catalysts are conventionally synthesized by wet impregnation of suitable oxide supports with an aqueous solution of ammonium heptamolibdate $(NH_4)_6Mo_7O_{24}$, followed by calcination at temperatures above 823 K [6]. In some cases molybdenum organometallic complexes such as $Mo(\eta^3\text{-Pr})_4$, $Mo_2(\eta^3\text{-Pr})_4$, $[Mo_2(OAc)_5]_2$ or $MoBu_4$ with labile ligands, able to coordinate central ions with three donor atoms (hapticity η^3), are also used as precursors [6,7]. Grafting of volatile precursors, like $MoCl_5$, on the carrier surface is another frequently used method suitable for preparing supported Mo-based catalysts. Deposited precursor reacts with hydroxyl groups of the support, giving rise to the surface oxomolybdenum species [8]. Classical methods however lead to strong heterogeneity of the surface MoO_x entities. Depending on the molybdenum loading, usually isolated and polymeric entities of various nucleation degree, as well as nanocrystalline MoO_3 forms can coexist on the support surface.

Recently, it was found that, despite relatively low solubility of MoO_3 in water (*i.e.* 0.1 g of MoO_3 per 100 g of H_2O), it is possible to use its slurry as an impregnating agent to obtain supported systems, exhibiting enhanced homogeneity of the deposited molybdenum. The latter property remains of vital importance for catalytic selectivity. Segregation of the deposited molybdena into undesirable MoO_3 nanocrystals can thus be avoided. Moreover, as no molecular molybdenum precursor is used in this method, calcination step, usually indispensable to decompose the precursor into an active phase, can also be omitted. Up to now slurry deposition was applied for preparing the catalysts containing MoO_3 deposited on SiO_2, MgO, γ-Al_2O_3, ZrO_2 and on active carbon [9–12].

In this work the interaction of NO with the surface of MoO_x/t-ZrO_2 catalysts of various MoO_3 loading was examined

* Corresponding author. Tel.: +48 12 663 22 24; fax: +48 12 634 05 15.
E-mail address: adamski@chemia.uj.edu.pl (A. Adamski).

0920-5861/$ – see front matter © 2008 Elsevier B.V. All rights reserved.
doi:10.1016/j.cattod.2008.02.018

by EPR spectroscopy. Catalytic removal of noxious NO_x involves an activating adsorption of gaseous reactants over catalyst surface. Therefore it is necessary to characterize in detail the nature of specific interactions between surface sites and the reactant molecules adsorbed from the gas phase, participating in deNO_x process. Particular attention was devoted to changes in the valence state of molybdenum sites induced by low-temperature (77 K) NO adsorption in the absence or in the presence of O_2, and to the thermal evolution of the resultant surface monocoordinated η^1-{Mo–NO}^{x} complexes.

2. Experimental

Single phase tetragonal zirconia (t-ZrO_2) with surface area of 77 m^2/g, was prepared by modified precipitation method from an aqueous solution of $ZrOCl_2{\cdot}8H_2O$ (Aldrich) of 0.6 M at room temperature. The fresh precipitate was aged in the parent solution at 373 K for 48 h under reflux with a periodical supplementation of $NH_{3(aq)}$ to keep constant pH ≈ 9. The resultant zirconia gel was dried at 373 K for 24 h, and finally calcined in air at 873 K for 6 h [13,14].

Slurry deposition method consisted in shaking the t-ZrO_2 support with the defined amount of MoO_3 (equivalent to 0.2–5.0 mol%), suspended in small quantity of water, until the concentration of molybdenum in the parent solution became negligible. Water with a small portion of dissolved MoO_3 penetrated into the pores of the support, where an equilibrium adsorption took place [15,16]. In the last stage of synthesis the final catalyst was dried at 393 K for 12 h. In the slurry deposition no precursor of the active component was used, because MoO_3, constituting an active phase, was directly contacted with the support material. Calcination, applied very often to decompose a precursor of an active phase into final oxide, can thus be eliminated. Detailed structural and spectroscopic characterization of a series of MoO_x/t-ZrO_2 catalysts obtained by slurry deposition will be a subject of a separate paper [17].

Gaseous reactants were adsorbed at the pressure of 2–20 Torr on samples previously outgassed at $p \leq 10^{-5}$ Torr and activated at 623–673 K for 0.5 h. The MoO_x/t-ZrO_2 samples were contacted with NO and O_2 at 77 K for 2 min and next gradually exposed to elevated temperatures, to follow the adsorption progress, monitored by EPR. CW-EPR X-band spectra were recorded at room and liquid nitrogen (77 K) temperatures with a Bruker ELEXSYS E-500 spectrometer. EPR parameters were determined by computer simulation using the EPRsim32 program [18]. In all reported cases spectral intensity was calculated as double integral.

3. Results and discussion

3.1. Reduced MoO_x/t-ZrO_2 catalysts

Regardless the content of MoO_3, the as-prepared samples were EPR silent, indicating that all molybdenum was present in the form of Mo^{6+} ions. It corresponds well to the fact that in the slurry deposition the calcination step is omitted and no reduction of surface molybdenum by decomposition products of the usually used $(NH_4)_6Mo_7O_{24}$ precursor, such as NH_3 or NO, takes place. In consequence, the presence of the paramagnetic Mo^{5+} ($4d^1$) ions was not revealed by EPR. For some samples a weak narrow EPR signal around g_{av} = 1.97, without any appreciable hyperfine (hf) structure, was observed at 77 K. It can be attributed to Zr^{3+} ($4d^1$) matrix defects [19]. Contrary to this, annealing the MoO_x/t-ZrO_2 samples at 573 K for 0.5 h in vacuum of 10^{-5} mbar, led to the appearance of a strong axial EPR signal at g_{av} = 1.93. The spectra recorded at 77 K for samples containing 0.2, 1.0 and 5.0 mol% of MoO_3 are shown in Fig. 1a–c. The observed signals are characteristic of Mo^{5+} ions in oxide environment [8,20]. Partial thermal reduction of the surface Mo^{6+} ions can be described by the equation, $MoO_3 \rightarrow [(Mo_{Mo})_{1-2x}(Mo'_{Mo})_{2x}]O_{3-x}(V_O^{\bullet\bullet})_x + 1/2O_2$, where Mo_{Mo} stands for Mo^{6+}, Mo'_{Mo} for Mo^{5+} and $V_O^{\bullet\bullet}$ for the positively charged oxygen vacancy (in Krőger–Vink notation) [21]. There are only two resolved hyperfine lines in the spectra (marked with arrows in Fig. 1), originating from the interaction of the unpaired electron with ^{95}Mo and ^{97}Mo nuclei (both with I = 5/2, and natural abundance of 15.70 and 9.46%, respectively). As it can be inferred from the shape of the 3rd derivative of the spectrum c, shown in the insert of Fig. 1, several molybdenum sites contributed to this EPR signal. Beside a small (below 15%) contribution of the polymeric MoO_x entities observed for MoO_3 loadings exceeding 1 mol% and giving rise to the structureless signal at g_{av} = 1.93, computer simulation confirmed the presence of at least three types of Mo^{5+} centers with $g_\perp^{(1)} = 1.972$, $g_\perp^{(2)} = 1.946$ and $g_\perp^{(3)} = 1.925$, which can be attributed to penta-, hexa- and tetra-coordinated surface sites, respectively [20,22].

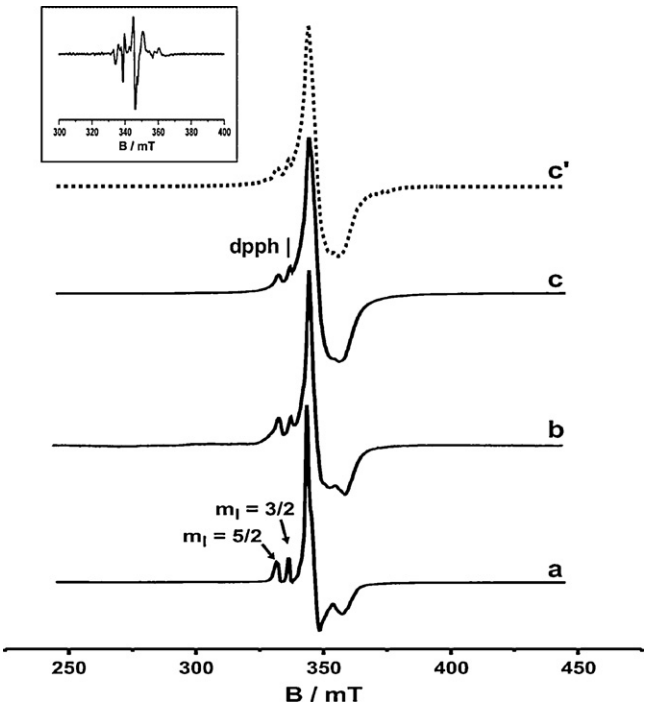

Fig. 1. EPR spectra of MoO_x/t-ZrO_2 catalysts containing: (a) 0.2, (b) 1.0 and (c) 5.0 mol% of MoO_3. Computer simulation of spectrum c is shown as c′. In the insert: third derivative of spectrum c is presented.

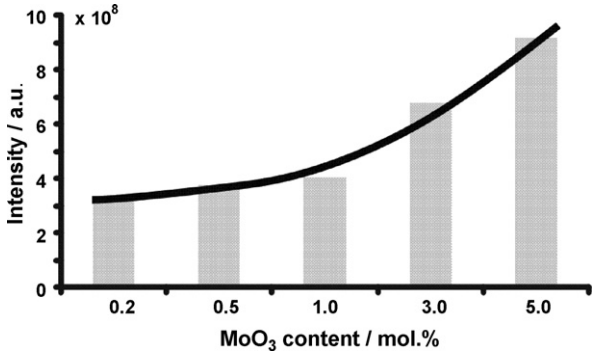

Fig. 2. Changes in the total spectral intensity (calculated as double integral of the first derivative spectra) vs. nominal MoO_3 loading (the line shown in this figure is just a guide for the eye).

The differences in both the spectral shape and the integral intensity, observed with the increasing MoO_3 loading, reflected a progressive increase of the content of Mo^{5+} ions in the investigated samples (Fig. 2). The changes in the intensity were much more pronounced in the case of Mo-rich samples (>1 mol%), where the contribution of polymeric MoO_x entities prevailed, than in the case of Mo-lean samples (<1 mol%), where isolated molybdenum species dominated. Broadening of the EPR spectra, leading to partial disappearance of the hyperfine lines, was caused by the growing dipol–dipol interactions between the Mo^{5+} sites, as their concentration increased.

3.2. Low-temperature NO adsorption on MoO_x/t-ZrO_2 catalyst

In the gas state, NO ($^2\Pi_{1/2}$) molecules are EPR silent. However, upon adsorption, due to removal of the degeneracy of both $2\pi^*$ orbitals, NO molecule gives rise to an orthorhombic **g**-tensor with $g_x = g_e + 2(\lambda/\Delta) - (\lambda/\delta)^2 + (\lambda/\delta)(\lambda/\Delta)$, $g_y = g_e - (\lambda/\delta)^2 - (\lambda/\delta)(\lambda/\Delta)$ and $g_z = g_e - 2(\lambda/\delta) + (\lambda/\delta)^3$, where λ is the spin–orbit coupling constant, and Δ and δ, the crystal field splitting parameters [23].

Low-temperature (77 K) contact of the MoO_x/t-ZrO_2 catalysts with 2–20 Torr of NO led to distinct changes in the EPR spectra. In Fig. 3A and B the results obtained before and after NO adsorption at p_{NO} = 2 Torr onto Mo-lean (0.2 mol%) and Mo-rich (5.0 mol%) samples, respectively, are shown. In both cases no new signal attributable to NO could be observed just after introduction of the gas onto the samples, and only a 2-fold increase in the intensity of the Mo^{5+} signal took place (*cf.* inserts in Fig. 3A and B). This can be explained by the partial reduction of the Mo^{6+} ions, accompanying the formation of η^1-{Mo^{5+}–NO^+}^{1} complexes. Subsequent exposure of the samples to the room temperature resulted in a progressive decrease of the intensity of the observed Mo^{5+} signals, possibly due to the further interaction of molybdenum sites with gaseous NO *via* spin-pairing mechanism, according to the equation:

$$NO(^2\Pi) + Mo^{5+}(^2D) \rightarrow \eta^1\text{-}\{Mo{-}NO\}.$$

In consequence, diamagnetic mononitrosyl adducts were produced. Redistribution of electron density between NO ligand and the metal ion determines, whether or not this process can be regarded as a formal reduction of Mo sites. If, in the formed

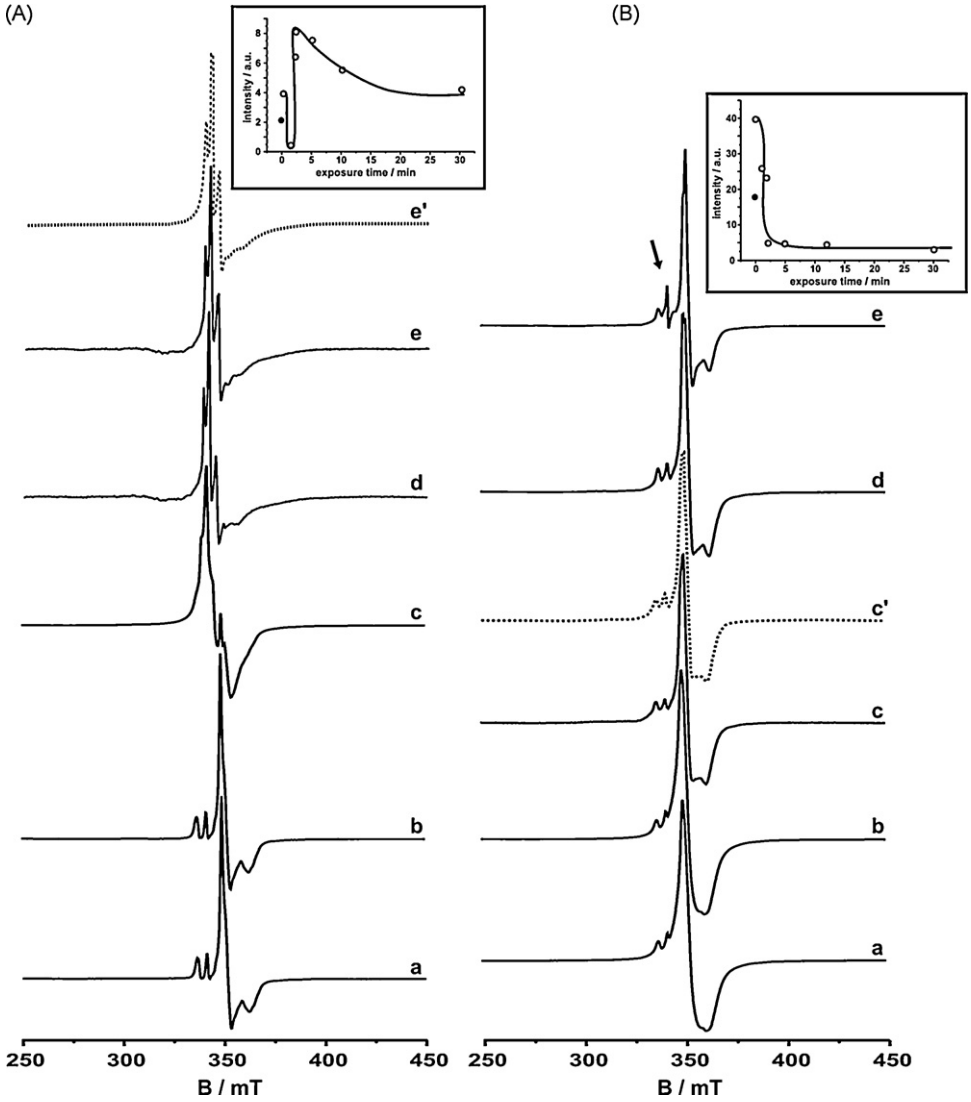

Fig. 3. Evolution of the normalized EPR spectra of MoO_x/t-ZrO_2 catalysts containing: (A) 0.2 mol% and (B) 5.0 mol% of MoO_3 (a) before and (b) after low-temperature NO adsorption (77 K, p_{NO} = 2 Torr) and subsequent exposure to (c) RT for 30 s, (d) 348 K for 10 min and (e) 503 K for 10 min; (c′) and (e′) corresponding simulated spectra. In the inserts: changes in the spectral intensity before and after NO adsorption. The black dots stand for the intensities of Mo^{5+} signals before NO introduction onto the samples of 0.2 and 5.0 mol% MoO_3.

complex, the electron density is mainly localized on the Mo moiety, this corresponds to the reduction of molybdenum centers from Mo(V) to Mo(IV). Nitric oxide activation over highly loaded molybdena catalysts was accompanied by changes in molybdenum speciation, as it can be inferred from the comparison of spectra b and c in Fig. 3B. Based on the results of computer simulation of the spectrum c (shown as c′), it can be stated that the components assigned to polymeric MoO_x ($g_{av} = 1.93$) and to the tetra-coordinated molybdenum ($g_{\perp} = 1.925$) disappeared after NO adsorption. Therefore no characteristic shoulder can be observed in the lower part of the spectrum. Two other components (at $g_{\perp} = 1.972$ and 1.946) were still present in the spectrum c, however their partial intensities were *ca.* 0.6 times lower. This fact indicates that the attack of NO was preferentially directed to the low-coordinated and more easily reducible molybdenum ions.

In the case of the samples containing the low amount of MoO_3 ($\leq$0.2 mol%), the adsorbed NO can also be stabilized on the zirconium surface sites (Fig. 3A). After 30 s of the NO interaction with the sample containing 0.2 mol% of MoO_3, a characteristic EPR signal of nitric oxide, chemisorbed on Zr^{4+} sites, with the emerging hyperfine structure due to the coupling of the unpaired electron with ^{14}N was observed (Fig. 3A, c–e). Its parameters, determined by computer simulation (spectrum e′), were quite similar to that one reported for {NO–$Ce_{0.75}Zr_{0.25}O_2$}, where isolated nitrosyl complexes coexisted with coupled (dimeric) nitrosyls [24]. The orthorhombic signal with $g_x = 1.989$, $g_y = 2.001$ and $g_z = 1.921$ and $|^{N}A_x|g\beta_e = 3.2$ mT can thus be attributed to the ligand-centred η^1-{Zr–NO}^{1} radical complexes. The resolution of the corresponding EPR signal was distinctly improved by the temperature increase to 503 K for 10 min (Fig. 3A, e), making the three-line hyperfine splitting due to ^{14}N ($I = 1$) clearly visible.

Evolution of the spectral intensity, shown in the insert to Fig. 3A, suggested two different modes of NO stabilization on the Mo-lean catalysts. Just after NO admission, the {Mo–NO}^{x} surface complexes were formed, that was accompanied by an increase and then quick decrease of the spectral intensity with exposure time, similar to that observed for Mo-rich catalysts. When the reaction of NO with Mo sites was accomplished, the remaining part of NO molecules interacted with Zr^{4+} centers, forming {Zr–NO}^{1} complexes, giving rise to an EPR signal with $g_x \approx 1.989$, $g_y \approx 2.001$ and $g_z \approx 1.921$ described above. Thus, two different types of adsorption centers coexisted at low concentration of surface molybdenum, making possible the competition between Mo and Zr sites as stabilization centers for NO molecules. The intensity of the corresponding EPR spectrum increased during the first 5 min of the exposure to room temperature and then slowly decreased in the same manner as it was previously observed for {NO–$Ce_xZr_{1-x}O_2$} complexes [25]. The signals of {Mo–NO}^{1} and {Zr–NO}^{1} appeared consecutively in the EPR spectra recorded as a function of exposure time, indicating that molybdenum sites play the role of the preferential activation centers for adsorbed NO molecules. In the case of Mo-rich samples, NO was adsorbed on molybdenum sites exclusively and no signal due to the formation of {Zr–NO}^{1} was observed.

High-temperature (503 K) interaction of NO with MoO_x/t-ZrO_2 catalyst, containing 5 mol% of MoO_3, led to the appearance of the new signal at $g \approx 2.0$ (Fig. 3B, e). Its attribution cannot be done univocally without more advanced investigations, but the lack of the hyperfine splitting from nitrogen suggested that, tentatively, this signal can be assigned to the paramagnetic oxygen-bearing species (see below). To verify this hypothesis dioxygen was adsorbed at 77 K on the same sample and the evolution of the resultant surface complexes was monitored by EPR.

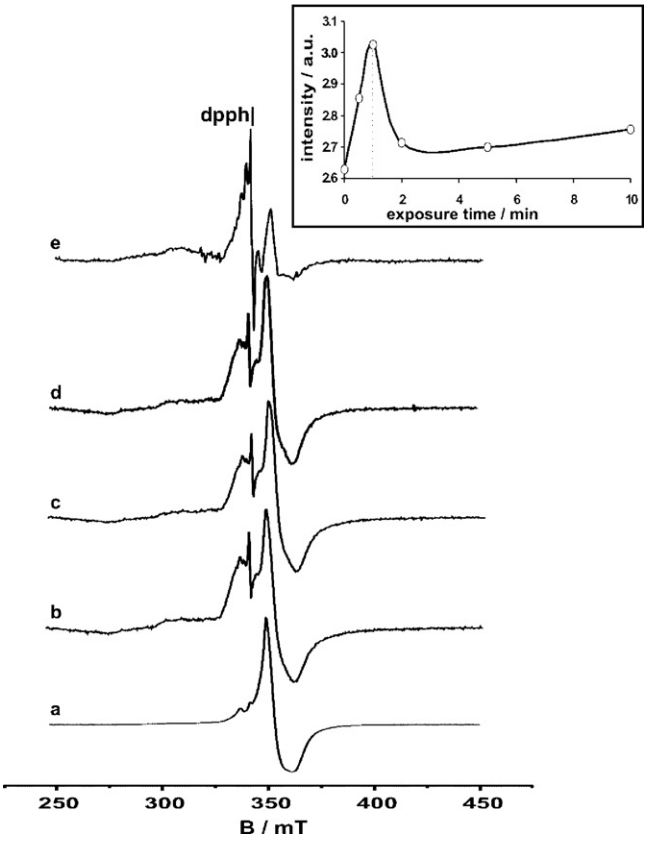

Fig. 4. The sequence of the EPR spectra of MoO_x/t-ZrO_2 catalyst containing 5.0 mol% of MoO_3 (a) before and (b) after low-temperature O_2 adsorption ($p_{O_2} = 2$ Torr) and subsequent exposure to (c) RT for 1 min, (d) RT for 10 min and (e) 573 K for 10 min. In the insert: changes in the intensity of the signal attributed to O_2^- species drawn as a function of time of exposure to RT.

3.3. O_2 activation over MoO_x/t-ZrO_2 catalysts

Adsorption of O_2 under the pressure of $p_{O_2} = 2$ Torr at 77 K on the Mo-rich samples led to the appearance of a new orthorhombic EPR signal at $g \approx 2.01$ (Fig. 4b), slightly overlapping with the lines of the molybdenum hyperfine structure. However, careful inspection of the relevant fragment of the EPR spectrum permitted us to distinguish between the signals originating from both paramagnetic centers. The parameters ($g_1 = 2.018$, $g_2 = 2.008$ and $g_3 = 2.004$) of the new signal suggested its attribution to the superoxide O_2^- ($^2\Pi_{3/2}$) anion-radical, stabilized within the coordination sphere of the molybdenum sites [26,27]. Formation of O_2^- on the reduced Mo centers requires an electron transfer from Mo^{5+} to the adsorbed dioxygen molecule (MLET), according to the equation: $O_2(^3\Sigma) + Mo^{5+}(^2D) = \{Mo^{6+}{-}O_2^-\}^1$. In consequence, a decrease in the intensity of the Mo^{5+} signal was observed during prolonged exposure of the sample to room and higher temperatures (Fig. 4c–e). Dioxygen activation occurred rather fast during O_2 chemisorption over catalysts surface, as it can be inferred from the evolution of the O_2^- signal intensity at room temperature (insert to Fig. 4). The maximum of its intensity was reached just after 1 min of the exposure, and the subsequent distinct decrease in the intensity of the O_2^- signal reflected transformation of superoxide radicals into diamagnetic O_2^{2-} and O^{2-} species as it was discussed in more detail elsewhere [28].

The role of O_2^- anion-radical in the low-temperature NO activation was examined in an additional experiment where 2 Torr of NO was introduced at 77 K onto MoO_x/t-ZrO_2 sample just after

the thermal evolution of the preadsorbed oxygen has been accomplished. The signal due to oxygen radical completely disappeared and no signal of NO appeared in the corresponding EPR spectrum. Apparently NO molecules spontaneously recombined with O_2^- species to form NO_3^- as final diamagnetic products of oxidation process, giving rise to the IR bands in the range of 1295–1625 cm^{-1} [29]

4. Conclusions

Interaction of NO with the surface of partially reduced MoO_x/t-ZrO_2 catalysts with low (0.2 mol%) and high (5.0 mol%) molybdenum loadings, obtained by slurry deposition, was studied by EPR spectroscopy. Formation of the paramagnetic η^1-{Mo^{5+}–NO^+}^{1} complexes was shown for both investigated systems, regardless the initial MoO_3 content. On molybdena-lean samples, NO can also be stabilized on the support Zr^{4+} sites in the form of η^1-{Zr–NO}^{1} mononitrosyls. Low-temperature contact of the catalyst containing 5.0 mol% of MoO_3 with O_2 led to the partial oxidation of reduced molybdenum and dioxygen activation into O_2^- paramagnetic species. The appearance of the reactive superoxide anion-radicals can be directly responsible for the formation of diamagnetic nitrates in course of the SCR NO_x process.

Acknowledgements

The authors are grateful to M.S. Paweł Jakubus from Institute of Chemistry and Environment Protection of Szczecin Technical University for providing us kindly a series of MoO_x/t-ZrO_2 samples. The work was performed in the framework of the project no. PBZ-MEiN-3/2/2006.

References

[1] J.-Sh. Chung, R.L. Burwell Jr., J. Catal. 116 (1989) 519.
[2] F.C. Meunier, A. Yasmeen, J.R.H. Ross, Catal. Today 37 (1997) 33.
[3] J. Haber, Molybdenum compounds in heterogeneous catalysis, in: E.R. Braithwaite, J. Haber (Eds.), Stud. Inorg. Chem., vol. 19, Elsevier, Amsterdam, 1994
[4] P. Forzatti, Appl. Catal. B 222 (2001) 221.
[5] G. Busca, L. Lietti, G. Ramis, F. Berti, Appl. Catal. B 18 (1998) 1.
[6] M.A. Bañares, H.C. Hu, I.E. Wachs, J. Catal. 150 (1994) 407.
[7] K. Marcinkowska, L. Rodrigo, S. Kaliaguine, P.C. Roberge, J. Catal. 97 (1986) 75.
[8] C. Louis, M. Che, M. Anpo, J. Catal. 141 (1993) 453.
[9] X. Ma, J. Gong, X. Yang, Sh. Wang, Appl. Catal. 280 (2005) 215.
[10] T. Klicpera, M. Zdražil, Catal. Lett. 58 (1999) 47.
[11] E. Hillerová, M. Zdražil, Appl. Catal. A 138 (1996) 13.
[12] J. Gong, X. Ma, X. Yang, Sh. Wang, N. Gao, D. Wang, Catal. Lett. 99 (2005) 187.
[13] P. Jakubus, A. Adamski, M. Kurzawa, Z. Sojka, J. Therm. Anal. Calorim. 72 (2003) 299.
[14] A. Adamski, P. Jakubus, Z. Sojka, Nukleonika 51 (Suppl. 1) (2006) S27.
[15] M. Zdražil, Catal. Today 65 (2001) 301.
[16] E. Hillerová, H. Morishige, K. Inamura, M. Zdražil, Appl. Catal. A 156 (1997) 1.
[17] A. Adamski, P. Jakubus, P. Zapała, Z. Sojka, to be published.
[18] T. Spalek, P. Pietrzyk, Z. Sojka, J. Chem. Inf. Model. 45 (2005) 18.
[19] M.J. Torralvo, M.A. Alario, J. Soria, J. Catal. 146 (1994) 335.
[20] M. Che, C. Louis, Z. Sojka, J. Chem. Soc., Faraday Trans. 1 (85) (1989) 3939.
[21] S.K. Deb, J.A. Chopoorian, J. Appl. Phys. 37 (1966) 4818.
[22] Z. Sojka, K. Dyrek, P.C. Roberge, M. Che, Pol. J. Chem. 65 (1991) 637.
[23] A. Volodin, D. Biglino, Y. Itgaki, M. Shiotani, A. Lund, Chem. Phys. Lett. 327 (2000) 165.
[24] A. Adamski, G. Djéga-Mariadassou, Z. Sojka, Catal. Today 119 (2007) 120.
[25] A. Adamski, E. Tabor, B. Gil, Z. Sojka, Catal. Today 119 (2007) 114.
[26] S.R. Seyedmonir, R.F. Howe, J. Chem. Soc., Faraday Trans. 1 (80) (1984) 2269.
[27] M. Che, A. Tench, Adv. Catal. 32 (1983) 1.
[28] M. Che, Z. Sojka, Topics Catal. 15 (2001) 211.
[29] K.I. Hadjiivanov, Catal. Rev. Sci. Eng. 42 (2000) 71.